University of Montana

ScholarWorks at University of Montana

Graduate Student Theses, Dissertations, & Professional Papers

Graduate School

1987

Nature and origin of bentonites and potassium bentonites northwestern Montana

Susan Claire Walker
The University of Montana

Follow this and additional works at: https://scholarworks.umt.edu/etd

Let us know how access to this document benefits you.

COPYRIGHT ACT OF 1976

THE NATURE AND ORIGIN OF BENTONITES AND POTASSIUM BENTONITES,

NORTHWESTERN MONTANA

By

Susan Claire Walker
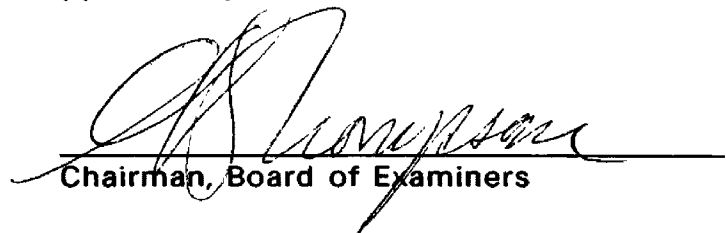
B.S., University of Miami, 1983

Presented in partial fulfillment of the requirements for the degree of

Master of Science

University of Montana
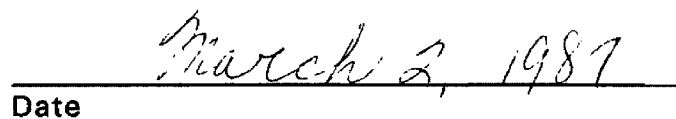
1987

Approved by

Chairman, Board of Examiners

Dean, Graduate school

Date

UMI Number: EP38386

UMI

Dissertation Publishing

UMI EP38386

ProQuest

ProQuest LLC.
789 East Eisenhower Parkway
P.O. Box 1346
Ann Arbor, MI 48106 - 1346

Low-grade metamorphic K-bentonites >1 meter (m) thick from the disturbed belt of western Montana show strong mineralogical and compositional zoning. The proportion of illite layers in illite/smectite (I/S) decreases progressively from the margins toward the centers of the beds. K-bentonites show progressive depletion of SiO_2 and progressive enrichment of K_2O from the centers of the beds outward to the shale contacts. Enclosing shales show enrichment of SiO_2 and some K_2O depletion adjacent the K-bentonite contacts. Mineralogic and compositional zoning is absent from age equivalent and genetically related unmetamorphosed bentonites from the Sweetgrass Arch and from thin K-bentonites in the disturbed belt.

Bentonites and K-bentonites of Late Cretaceous age in western Montana were mineralogically and chemically analyzed to develop an understanding of the processes by which they form. Normal smectite-rich bentonites from the Sweetgrass Arch form by the subaqueous alteration of volcanic ashes and become K-poor through early loss of alkalis and calcium. I/S-rich K-bentonites from the disturbed belt are the low-grade metamorphic products of normal bentonites. To convert smectite to an I/S in K-bentonites, layer charge increases by tetrahedral substitution of Al^{3+} for Si^{4+} in the smectite. Layer charge increase appears to be controlled by Si^{4+} diffusion rates out of the bed and consequent Al_2O_3/SiO_2 ratios in the K-bentonite. Collapse of high charge smectite layers to form illite layers occurs when K^+ diffuses into a bed from surrounding shales. Because of slow Si^{4+} diffusion out of the bed, thick (>1 m) K-bentonites are zoned with illite and K-rich contacts and smectite and Si-rich inner portions. Diffusion of Si^{4+} and K^+ is complete, or nearly so in mineralogically and compositionally homogeneous thinner K-bentonites. If sufficient K^+ is not available, high charge smectite layers remain expanded and results in three component mixed-layer (M-L) clays consisting of illite, smectite and vermiculite (high charge smectite).

ii

Table of Contents

List of Figures

List of Tables

ACKNOWLEDGEMENTS

Special thanks go to my thesis advisor Dr. Graham Thompson for providing consistent support and guidance, expert advice and criticism, as well as incentive toward completion of the thesis. Thanks also to Dr. James Sears and Dr. Keith Osterheld for providing valuable advice and guidance on the thesis.

A NORCUS appointment at Rockwell-Hanford in Richland, Washington facilitated chemical analyses for the bulk of my bentonite samples. Special acknowledgements go to Dr. Duane Horton and Dr. Jim Burnell at Rockwell-Hanford for acting as technical contacts during this appointment and Dale Marcy for acting as escort and chemical consultant. Dr. Peter Hooper at Washington State University provided x-ray fluorescence analyses.

I would also like to thank Paul McLeod, fellow graduate student and clay mineralogist, for sharing many inspirational and deeply religious discussions on clay mineralogy. Thanks go to Sue Purvis for assisting me with field work, sampling the "twenty-foot bed" and taking over my "Inspiration" job. Thanks also to Seth Brandenberger for leaving town in the nick of time.

INTRODUCTION

Vitric volcanic ashes deposited in marine environments alter to potassium-poor smectite-rich bentonites, which, under conditions of low-grade metamorphism, in turn alter to potassium-rich K-bentonites (Kiersch and Keller, 1955; Slaughter and Earley, 1965; Grim and Guven, 1969; Hoffman and Hower, 1979; Velde and Brusewitz, 1982; Altaner et al, 1984). I have examined mineralogy and chemistry of genetically related ash flow tuffs, bentonites and K-bentonites from age equivalent strata of the Elkhorn Mountains volcanics, the Sweetgrass Arch and the disturbed belt, respectively, of western Montana (Fig. 1) to develop a model for the processes associated with those transformations.

Volcanism occured in western Montana throughout much of Late Cretaceous time. Ash eruptions of the Elkhorn Mountains volcanics -- the extrusive mantle of the Boulder batholith -- deposited large volumes of ash flow tuffs and related volcanic rocks in the vicinity of the Boulder batholith (Watson, 1986). The distal facies of those volcanics were deposited in the Late Cretaceous seaway east of the rising Rocky Mountains as vitric air-fall and water worked ashes which now comprise the bentonites and K-bentonites of the Sweetgrass Arch and disturbed belt (Nascimbene, 1964).

The disturbed belt of western Montana consists physiographically of the Front Ranges and the foothills of the northern Rocky Mountains; it formed by thrusting of Paleozoic and Precambrian strata over the Mesozoic section during the

1

early Tertiary Laramide orogeny (Mudge, 1970). Late Cretaceous sediments of the disturbed belt were subjected to low-grade metamorphism due to burial beneath thrust sheets involving temperatures in the range of 100-200°C (Mudge, 1970; Hoffman and Hower, 1979). The relatively undisturbed Sweetgrass Arch lies approximately 50 kilometers to the east of the disturbed belt (Fig. 1). Stratigraphically equivalent Late Cretaceous units from the Sweetgrass Arch have been buried only to shallow depths. Assemblages present indicate surface or near-surface conditions with maximum temperatures $<<60°C$ (Hoffman and Hower, 1979).

Typical bentonites from the Arch are composed of pure smectite or very highly expansible mixed-layer illite/smectite (I/S) and have low K_2O contents. Typical K-bentonite beds from the disturbed belt are potash-rich and are composed of I/S of intermediate to high percent illite layers or of three component mixed-layer illite/smectite/vermiculite (I/S/V) of high average layer charge.

The ash units of the Elkhorn Mountains volcanics, the bentonites of the Sweetgrass Arch and the K-bentonites of the disturbed belt appear to preserve steps in the progressive development of bentonites from volcanic ashes and, in turn, K-bentonites from bentonites as the vitric ashes were deposited in and reacted with sea water and surrounding sediments, and later were exposed to low-grade metamorphism.
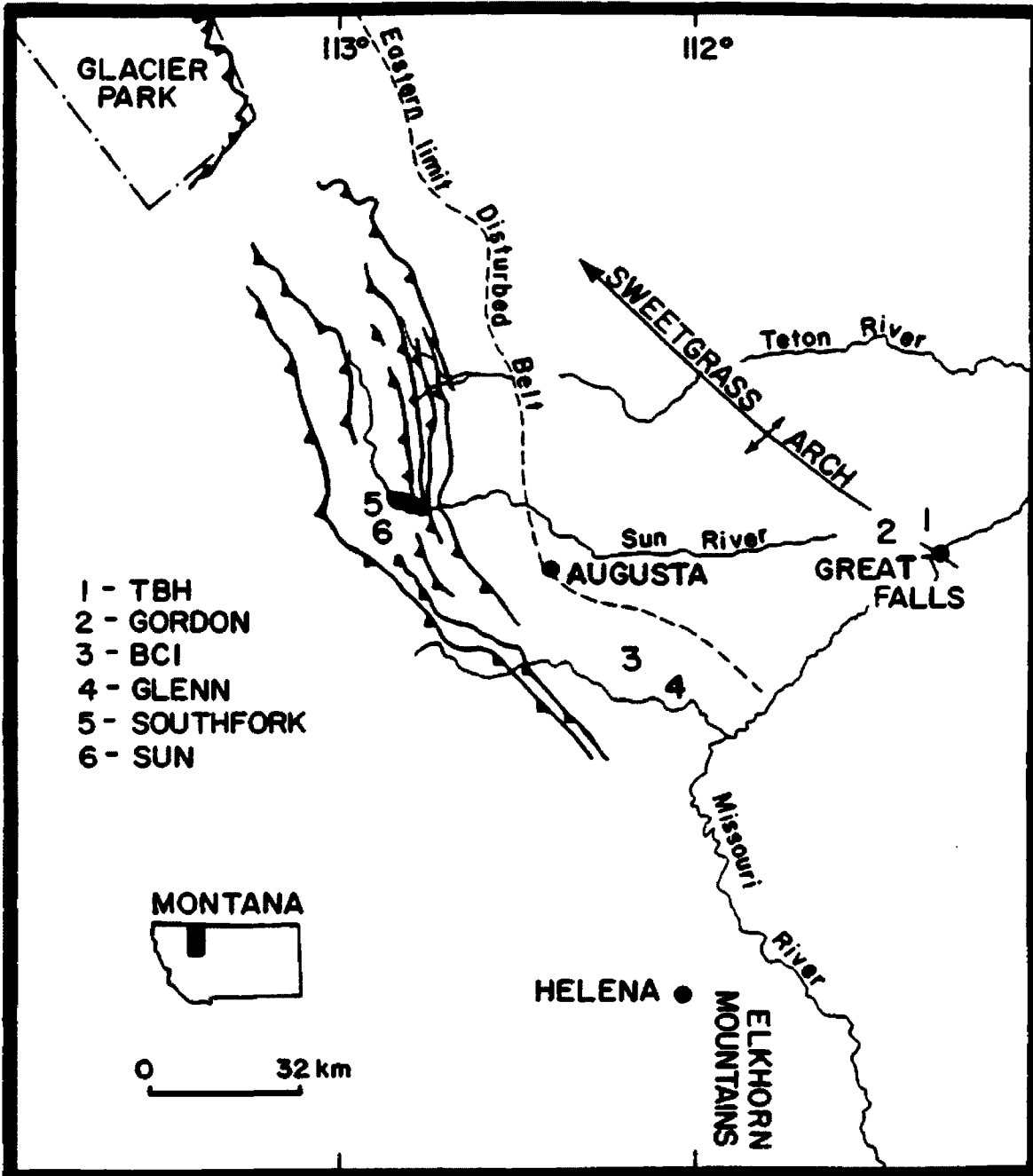
Figure 1 Sample Localities

METHODS

Sampling

Approximately sixty bentonite and K-bentonite units and associated mudrocks of Late Cretaceous age were sampled in western Montana. Samples were taken every 10 cm or less perpendicular to bedding across the bentonite and K-bentonite beds and for several meters out into enclosing shales. Two bentonites from the Sweetgrass Arch and four K-bentonites from the Disturbed Belt were chosen for more detailed analysis based on stratigraphic thickness and mineralogy. Sample localities for those six bentonites and K-bentonites are shown in Figure 1. Chemical analyses of ash flow tuff units from the Elkhorn Mountains volcanics were taken from Rutland (1985) and Watson (1986) and used for comparison with bentonite and K-bentonite compositions.

X-ray Diffraction Analysis

Samples were first crushed then disaggregated in deionized water with an ultrasonic probe. Samples were then separated into the <1 micron size fraction by centrifugation. The <.1 micron size fraction was separated from the <1 micron fraction by means of a Sharples continuous flow centrifuge (Jackson, 1956). Oriented sample mounts were prepared for XRD analysis by evaporation of 100 mg clay slurries onto glass slides. X-ray patterns were run on glycol-solvated oriented clay samples with a Philips Norelco x-ray diffractometer using CuKα

4

radiation and a graphite crystal monochrometer. Mineralogy of the bentonites was determined from the x-ray patterns of the <1 micron size fraction, and mineralogy of the shales from x-ray patterns of the <.1 micron size fraction. X-ray patterns were interpreted using the methods of Reynolds and Hower (1970) and Srodon (1981,1984).

To determine the presence of vermiculite, or high charge smectite, and other clay minerals, selected samples were progressively heated for 1 hour at 350°C, 450°C, 550°C, 650°C, with XRD runs at each stage. Samples were K^+ saturated with a 1N KCL solution followed by repeated washings and glycol solvation (Carroll, 1970). Samples were Mg^{2+} saturated then glycol and/or glycerol solvated (Brindley, 1966). K^+ saturation followed by Mg^{2+} saturation was used to determine if layer collapse with K^+ is irreversible. Selected samples were heated at 600°C for 1 hour, and treated with 1N HCL at 100°C for 1 hour to confirm the presence of kaolinite and/or chlorite.

Chemical Analysis

Fifty-eight samples from the six selected bentonites, K-bentonites and enclosing shales were chosen for bulk chemical analysis. Shale units below the bentonites were chosen for analyses to minimize the depositional reworking effects that might have mixed bentonite with the upper shale unit (Altaner, 1985). Most samples were fused with lithium metaborate, prepared according to the scheme outlined in Van Loon and Parissis (1966) and analyzed for silicon, aluminum, potassium, sodium, calcium, magnesium, iron, manganese and titanium

with an ARL-Inductively Coupled Argon-Plasma Spectrophotometer 3400-X. Analytic precision using ICP is: SiO_2, 0.83, Al_2O_3, 0.64, Fe_2O_3, 1.11, MgO, 1.08, K_2O, 1.11, CaO, 1.45, Na_2O, 1.42.

Other analyses were done by x-ray fluorescence with matrix corrections. Analytical precision using x-ray fluorescence is: SiO_2, 0.55, Al_2O_3, 0.31, Fe_2O_3, 0.35, MgO, 0.15, K_2O, 0.03, CaO, 0.22, Na_2O, 0.16.

DATA

Complete mineralogic and compositional data for all six bentonites, K-bentonites and enclosing shales are listed in Table 1. Figures 2-7 show mineralogic and compositional trends compared with stratigraphic position in the bentonites, K-bentonites and enclosing shales. Figures 2 and 3 show bentonites collected from the Sweetgrass Arch. Figures 4 and 5 show K-bentonites collected from near the eastern limit of the disturbed belt and Figures 6 and 7 show K-bentonites collected from deep within the disturbed belt. The whole rock chemical data for SiO_2 and K_2O are expressed as oxide ratios to Al_2O_3 because Al_2O_3 has an extremely low solubility and should have low chemical mobility (Altaner *et al*, 1984). Plots of other oxide trends are not shown because variations generally are non-systematic.

Sweetgrass Arch Bentonites

The TBH bentonite (Fig. 2) contains 100% expansible smectite and oxide trends show little or no systematic variation. The sample from the lower margin shows 5% illite layers in I/S (R=0) and a higher value of K_2O and somewhat lower value of SiO_2 than in the rest of the unit. Lower shale samples also show 5% illite layers in I/S (R=0), similar SiO_2 values to the bentonite, and a wide variation in K_2O values.

The GORDON bentonite (Fig. 3) shows I/S ranging from 35% I (R=0) at the

7

Table 1 Mineralogic and Compositional Data

SAMPLE	%IinI/S	ORD	SIO2	AL2O3	K2O	NA2O	CAO	MGO	FEO	TIO2	MNO
Sweetgrass Arch Bentonites and Shales(*)											

Sweetgrass Arch Bentonites and Shales(*)
TBH Bentonite- Bootlegger Member, Blackleaf Formation:
NW 1/4, Sec 17 R 4 E T 21 N, E. side of HWY 15

SAMPLE	%IinI/S	ORD	SIO2	AL2O3	K2O	NA2O	CAO	MGO	FEO	TIO2	MNO
TBH6A	0	R=0	72.03	18.86	.81	2.06	.51	1.81	3.69	.24	.003
TBH18C	0	R=0	72.01	18.46	.79	1.78	.59	1.61	4.52	.24	.005
TBH36F	0	R=0	72.71	18.44	.79	1.74	.48	1.68	3.99	.17	.004
TBH56I	0	R=0	75.58	16.96	.70	1.39	.40	1.39	3.39	.18	.004
TBHB/S	5	R=0	67.97	21.23	1.11	2.27	.82	1.96	4.40	.24	.004
TBHLS12*	5	R=0	70.69	20.41	.73	2.09	.72	1.65	3.52	.19	.004
TBHLS24*	5	R=0	76.39	16.32	.93	1.71	.45	.98	2.83	.39	.004

GORDON Bentonite- Vaughn Member, Blackleaf Formation:
S 1/2, Sec 27 R 1 E T 22 N, W. side of HWY 15

SAMPLE	%IinI/S	ORD	SIO2	AL2O3	K2O	NA2O	CAO	MGO	FEO	TIO2	MNO
GORD-1	35	R=0	60.34	20.11	2.04	2.10	6.14	1.90	6.92	.25	.213
GORD-8	17	R=0	62.40	25.17	2.07	2.58	.40	2.68	4.51	.18	.009
GORD-15	5	R=0	62.95	24.25	1.60	2.69	.40	2.96	4.94	.20	.014
GORD-21	17	R=0	62.14	24.82	1.75	2.80	.39	2.64	5.23	.22	.013
GORD-27	23	R=0	63.95	23.46	1.83	2.79	.58	2.92	4.21	.23	.029

Disturbed Belt K-Bentonites and Shales(*)
BCI K-Bentonite- Hogan Member, Two Medicine Formation:
Center, Sec 30 R 4 W T 18 N, S. Side HWY 200

SAMPLE	%IinI/S	ORD	SIO2	AL2O3	K2O	NA2O	CAO	MGO	FEO	TIO2	MNO
BCIL/R	72	R=1	58.38	26.53	5.95	.53	1.29	3.60	3.01	.70	.010
BCI18F	65	R=1	57.33	27.43	5.93	.18	2.46	3.65	2.37	.64	.016
BCI6A	72	R=1	57.73	27.55	6.11	.54	1.11	3.55	2.67	.74	.006
BCIU/L	75	R=1	63.50	22.14	4.58	1.10	1.22	3.23	3.48	.75	.011
BCILS/B*	90	R=3	74.12	14.77	3.19	1.43	.64	1.96	3.30	.60	.010
BCILS6A*	85	R=1	72.35	14.79	3.34	1.43	.69	2.31	4.48	.60	.010
BCILS18*	80	R=1	71.76	14.16	2.59	1.29	1.40	2.86	5.35	.57	.019

GLENN K-Bentonite- Hogan Member, Two Medicine Formation:
NW 1/4, Sec 22 R 4 W T 17 N, E. Side HWY 287

SAMPLE	%IinI/S	ORD	SIO2	AL2O3	K2O	NA2O	CAO	MGO	FEO	TIO2	MNO
GLENN/S	60	R=0	59.87	18.73	2.93	1.25	10.62	3.63	2.02	.59	.220
GLENN6A	35	R=0	64.87	21.10	2.81	.33	4.33	3.88	2.06	.56	.075
GLENN30	20	R=0	70.61	18.51	2.23	.23	1.59	3.97	2.30	.48	.013
GLENN66	15	R=0	73.38	16.20	2.00	.60	2.82	2.64	1.78	.45	.050
GLENN96	20	R=0	69.67	17.62	2.34	.34	4.82	3.34	1.37	.44	.065
GLENN114	20	R=0	54.93	16.44	2.50	.88	20.49	2.95	1.12	.44	.250
GLENN138	30	R=0	76.74	15.88	2.16	.41	.87	2.16	1.26	.45	.000

Table 1, continued

SAMPLE	%IinI/S	ORD	SIO2	AL2O3	K2O	NA2O	CAO	MGO	FEO	TIO2	MNO
GLENNSB*	I/S/V	-	76.36	15.13	2.23	.45	.83	2.59	1.99	.42	.011
GLENNS24*	33	R=0	73.79	17.12	2.32	.58	.92	3.12	1.68	.46	.010
GLENN144*	60	R=0	69.75	17.82	3.38	.76	.94	3.31	3.48	.55	.012
GLENN180*I/S/V		-	70.28	12.77	3.30	.90	4.76	4.02	3.45	.49	.030

SOUTHFORK K-Bentonite- Vaughn Member, Blackleaf Formation:
SE 1/4, Sec 27 R 10 W T 22 N, N. Bank of S. Fork Sun River

SAMPLE	%IinI/S	ORD	SIO2	AL2O3	K2O	NA2O	CAO	MGO	FEO	TIO2	MNO
SFORK105	80	R=1	68.52	20.19	4.26	.71	2.11	1.73	2.15	.25	000
SFORKP75	62	R=0	80.23	12.89	2.08	.55	1.65	.99	1.39	.16	000
SFORKK50	55	R=0	75.88	14.92	2.13	.72	2.76	1.27	2.06	.20	000
SFORKF25	65	R=0	77.65	15.11	2.50	.43	1.35	1.33	1.44	.15	000
SFORKD15	62	R=.5	76.76	15.73	3.06	.41	1.17	1.29	1.40	.15	000
SFORK1A1	65	R=.5	59.63	22.81	3.75	1.12	3.95	2.21	5.75	.54	.030
SFORKBA2*	95	R=3	79.13	9.67	2.08	.75	2.32	.85	4.60	.45	.010
SFORKE20*	95	R=3	68.95	12.67	2.86	1.13	5.84	1.75	5.97	.57	.050
SFORKF40*	95	R=3	66.50	12.47	2.93	1.17	7.98	2.29	5.75	.61	.060
SFORKG80*	95	R=3	69.76	17.32	4.07	.58	.88	1.53	4.89	.76	000
SFORK150*	95	R=3	70.64	17.83	4.05	.57	.22	1.19	4.51	.79	000

SUN K-Bentonite- Kevin Shale Member, Marias River Formation:
NE 1/4, Sec 34 R 10 W T 22 N, N. Bank of S. Fork Sun River

| SAMPLE	%IinI/S	ORD	SIO2	AL2O3	K2O	NA2O	CAO	MGO	FEO	TIO2	MNO
SUNUS66*	>80	R=3	66.67	14.14	3.34	.37	8.10	1.80	4.94	.62	.033
SUNUS46*	>80	R=3	73.28	14.53	3.43	.39	.40	1.60	5.73	.62	.022
SUNUS18*	>80	R=3	72.48	13.93	3.29	.47	2.17	1.98	5.13	.52	.027
SUNUS6A*	>80	R=3	74.01	12.24	2.76	.41	3.98	1.45	4.72	.40	.028
SUNUSO*	>80	R=3	72.49	15.21	2.95	.54	3.73	1.64	3.14	.26	.026
SUNBUS*	I/S/V	-	69.26	20.33	4.37	.60	1.42	1.77	1.95	.23	.000
SUNB6A	I/S/V	-	66.80	22.77	4.45	.37	1.20	2.36	1.91	.19	.003
SUNB24E	I/S/V	-	71.11	19.09	3.73	.34	1.27	2.22	2.06	.17	.004
SUNB54J	I/S/V	-	77.88	14.23	2.22	.34	1.47	1.75	1.96	.15	.005
SUNB66L	I/S/V	-	76.46	16.18	2.35	.26	1.21	1.81	1.60	.14	.003
SUNB84N	I/S/V	-	77.39	13.91	2.22	.45	2.23	1.70	1.93	.16	.009
SUNB960	I/S/V	-	71.90	17.64	3.46	.48	2.30	1.95	2.06	.19	.018
SUNBLS*	I/S/V	-	66.84	22.71	4.47	.28	1.21	2.37	1.94	.19	.004
SUNLSO*	>80	R=3	77.86	10.91	2.25	.76	2.01	1.21	4.55	.44	.016
SUNLS6A*	>80	R=3	77.78	10.04	2.09	.57	3.20	1.13	4.69	.45	.035
SUNLS18*	>80	R=3	73.76	10.41	2.44	.49	5.77	1.61	4.98	.47	.059
SUNLS46*	>80	R=3	69.64	12.78	3.02	.49	5.78	1.92	5.77	.55	.048
SUNLS56*	>80	R=3	68.54	14.15	3.18	.66	5.74	1.67	5.42	.58	.071
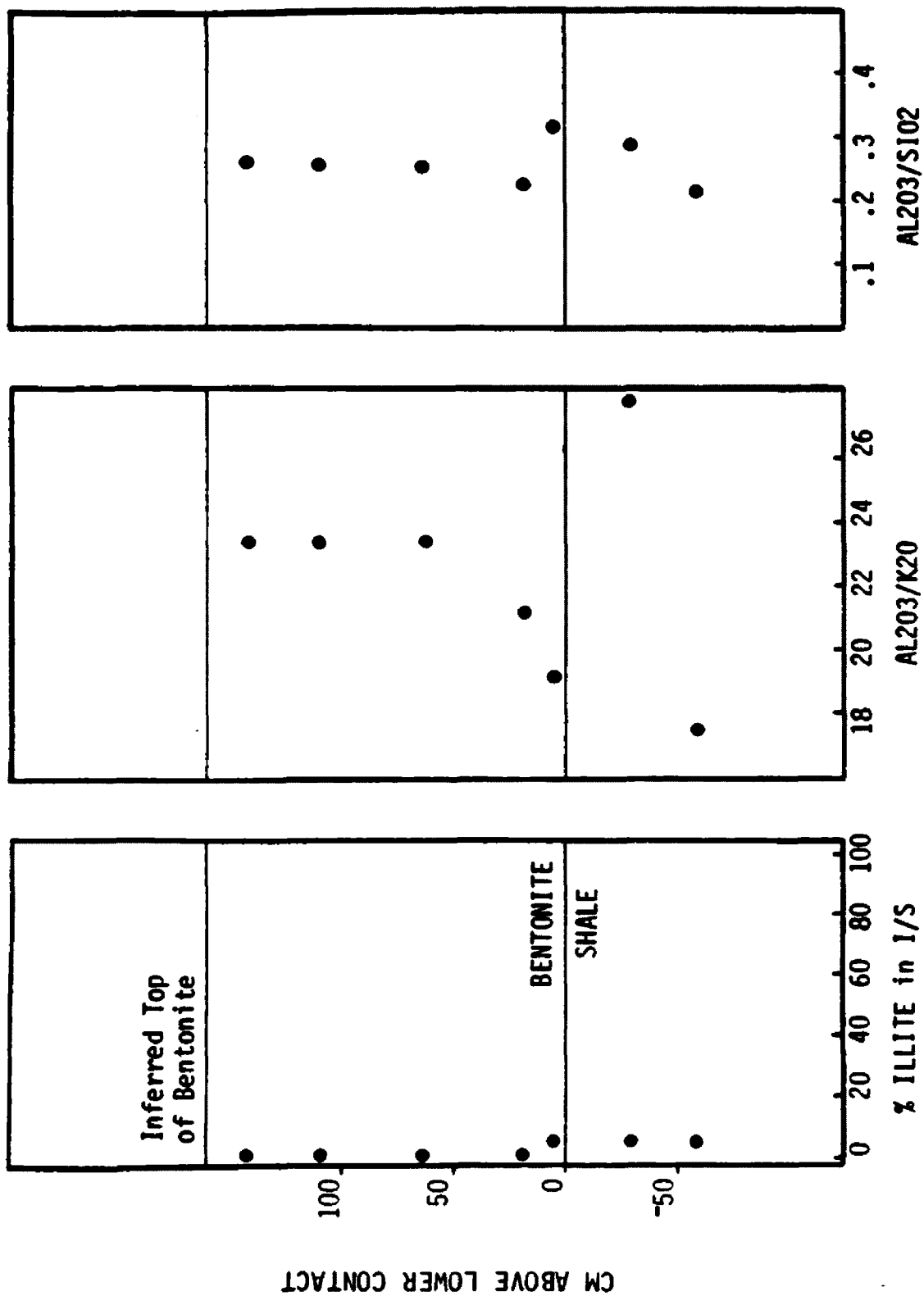
Figure 2. Mineralogy and Al_2O_3/K_2O and Al_2O_3/SiO_2 for the 1.42 m thick TBH Bentonite
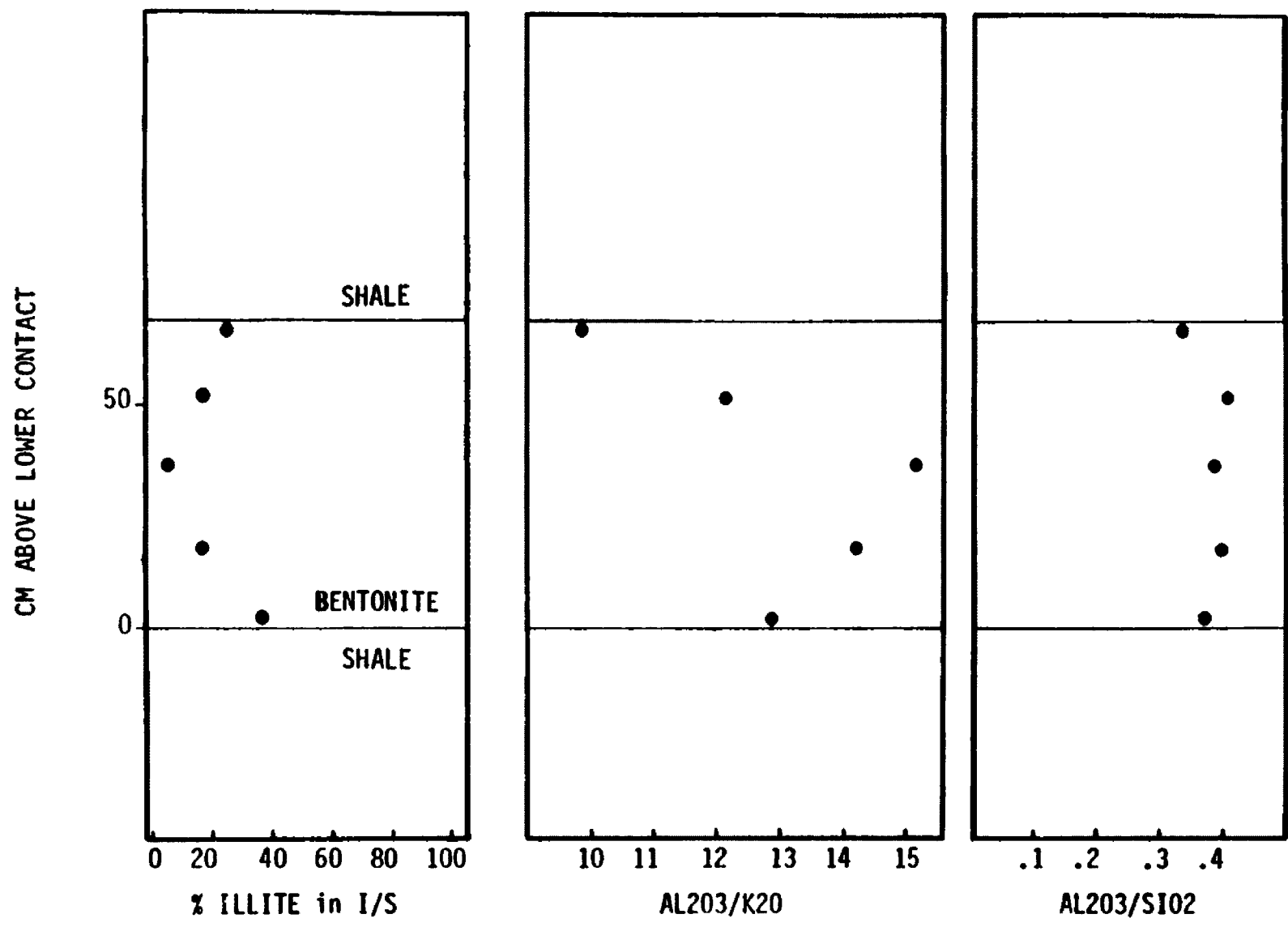
Figure 3. Mineralogy and Al_2O_3/K_2O and Al_2O_3/SiO_2
for the 0.75 m thick GORDON Bentonite

margins to 5% I (R=0) in the center. K_2O values are significantly higher, and SiO_2 slightly lower at the margins. No shale samples were collected with this bentonite.

Disturbed Belt K-bentonites

The BCI K-bentonite (Fig. 4) shows I/S ranging from 75% I (R=1) at the margins to 65% I (R=1) at the center. K_2O and SiO_2 values show little variation. Mineralogy of the shales shows 80-90% I in I/S (R=3) as well as some discrete illite and chlorite. K_2O values in the shale are similar to those in the K-bentonite and SiO_2 values are higher. Little compositional variation occurs in the shales.

The GLENN K-bentonite (Fig. 5) shows assymetric distribution of mineralogy, with I/S ranging from 60% I (R=0) at the upper margin, 15% I (R=0) in the center, and 30% I (R=0) at the lower contact. K_2O is higher and SiO_2 is lower, at the margins than in the center of the bed. Mineralogy of the shales shows 30-60% I in I/S (R=0) as well as some three component mixed-layer illite/smectite/vermiculite (by vermiculite I mean an expansible smectite-like mineral with a higher than normal charge for a smectite. This mixed-layer mineral will be discussed in the following section). K_2O varies in the shales with higher values away from the K-bentonite contact, and values similar to those in the K-bentonite nearer the contact. SiO_2 shows little variation across the shale.

The SOUTHFORK K-bentonite (Fig. 6) shows strong mineralogic and compositional zonation with I/S ranging from 80% I (R=1) at the margins to 55% I (R=0) in the center. K_2O is higher, and SiO_2 is lower at the margins than in the center of the bed. Mineralogy of enclosing shales show 95% illite in I/S (R=3) as
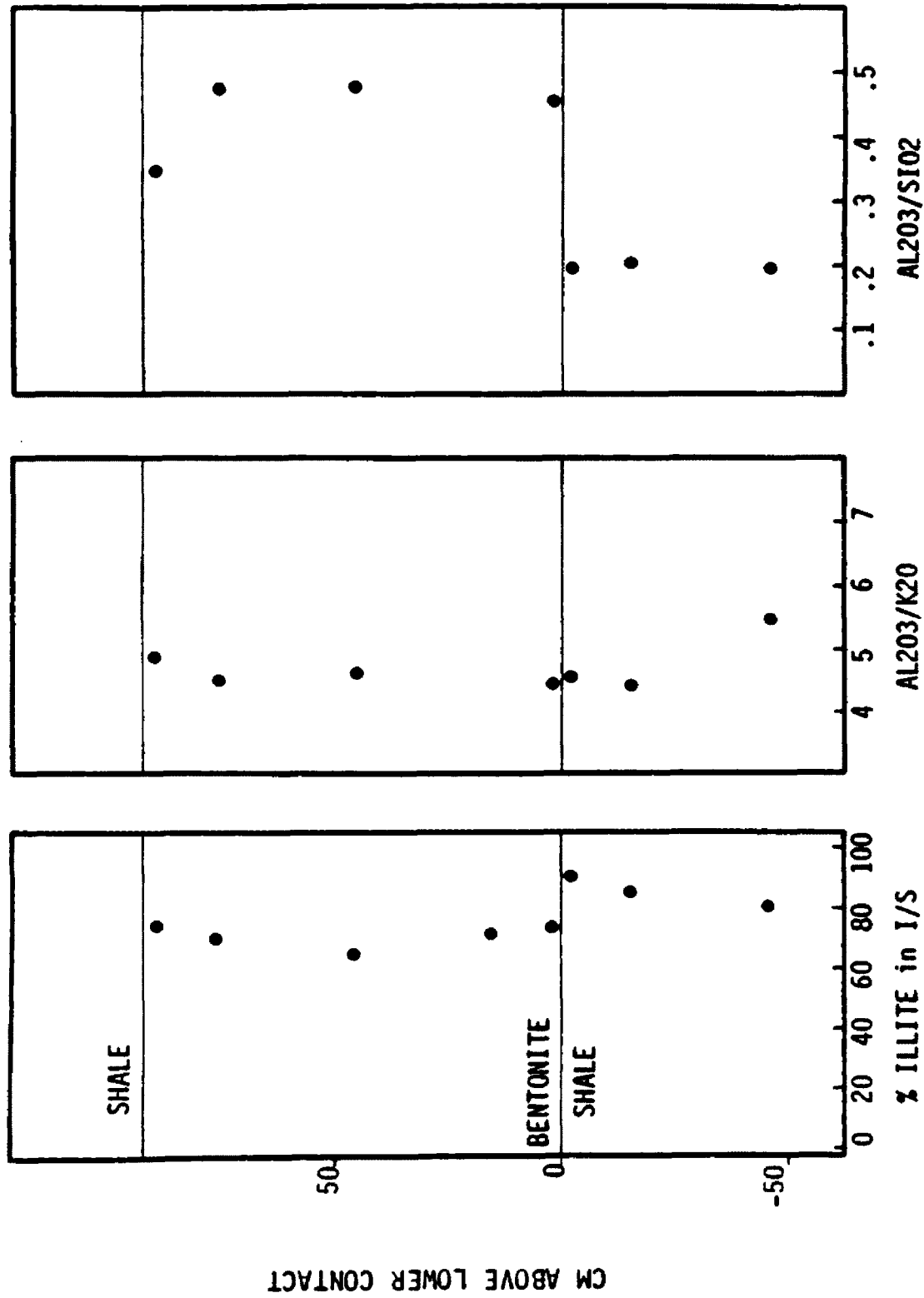
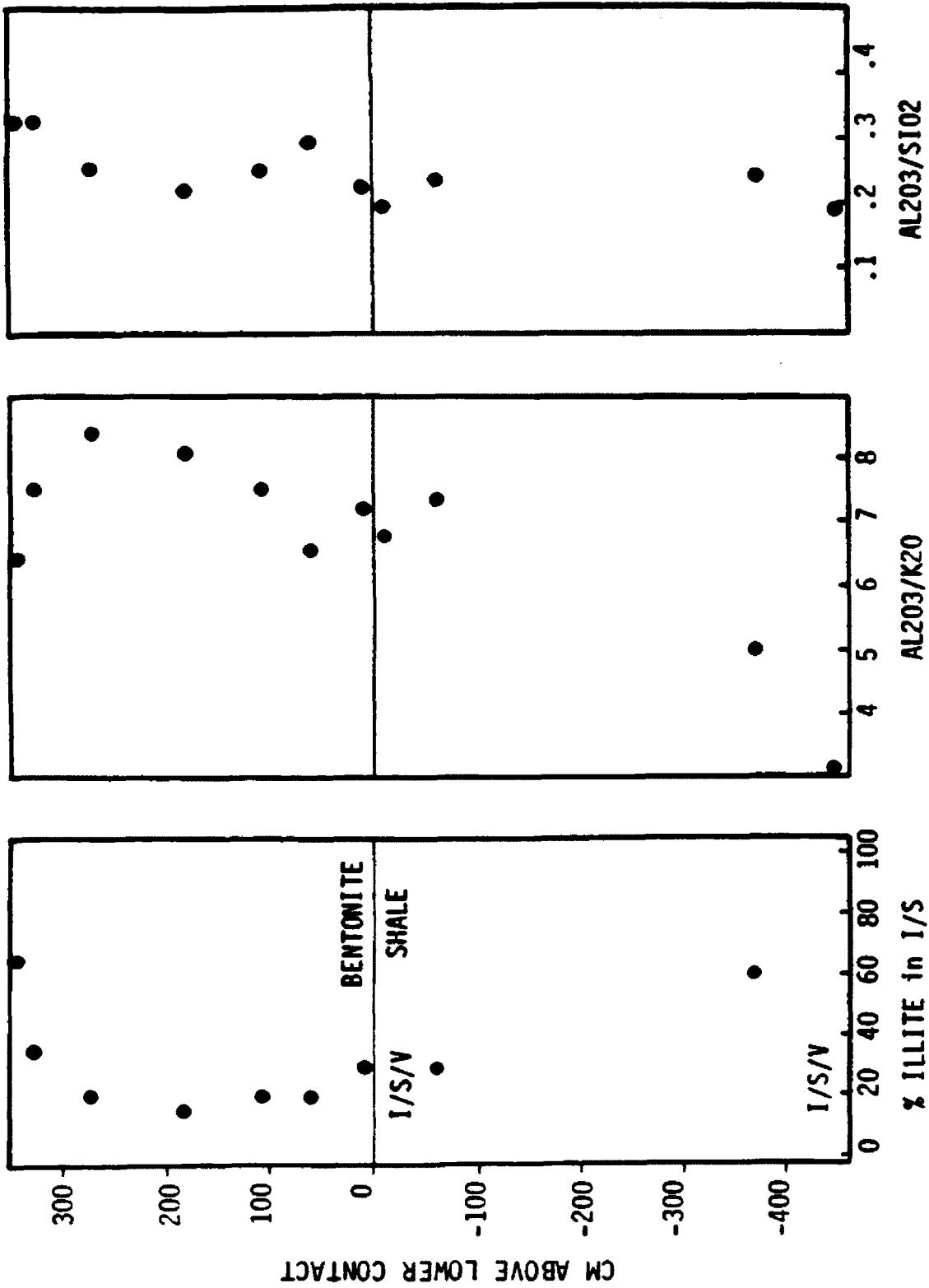Figure 4. Mineralogy and Al_2O_3/K_2O and Al_2O_3/SiO_2 for the 1.00 m thick BCI K-bentonite

Figure 5. Mineralogy and Al_2O_3/K_2O and Al_2O_3/SiO_2 for the 3.84 m thick GLENN K-bentonite
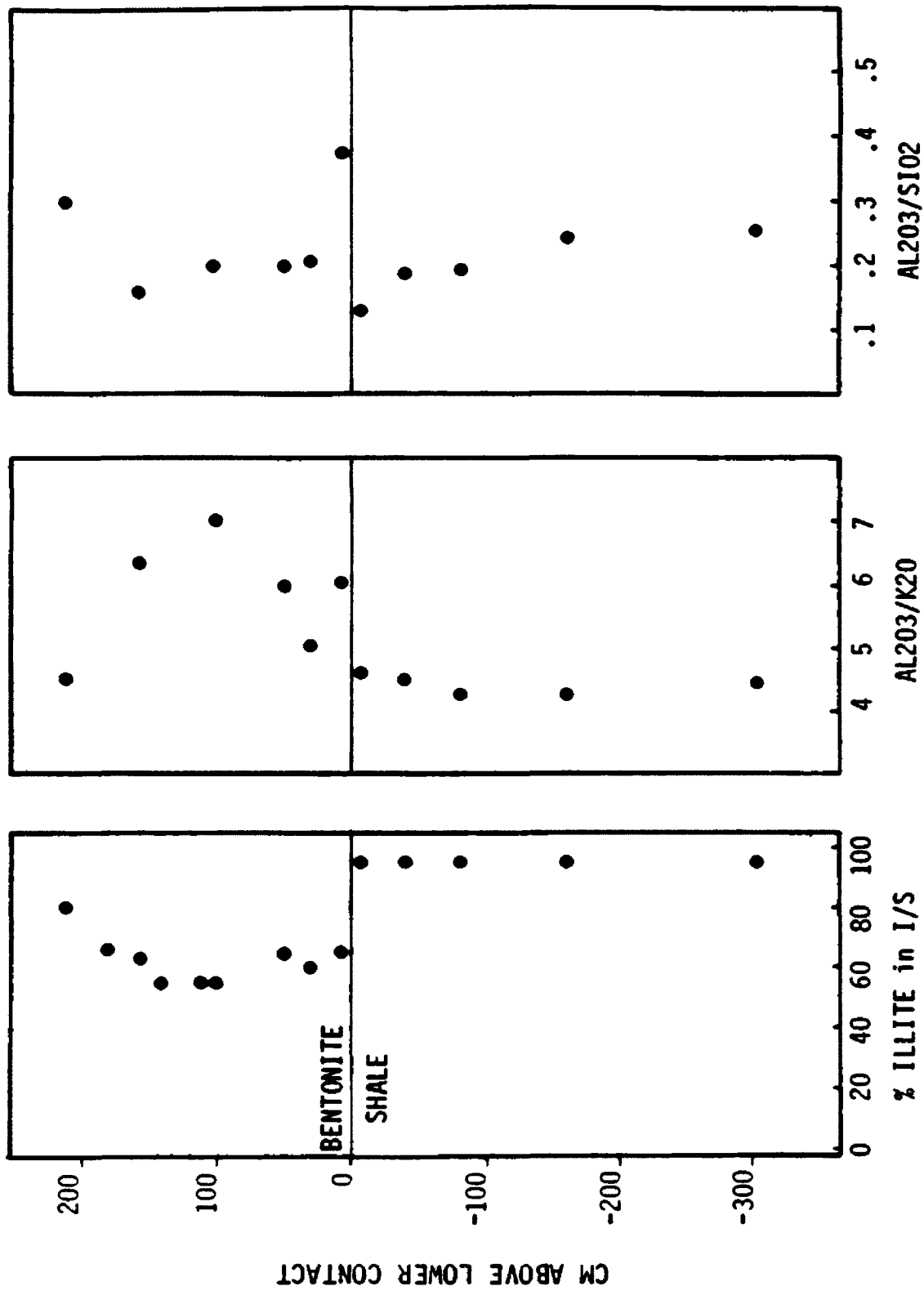
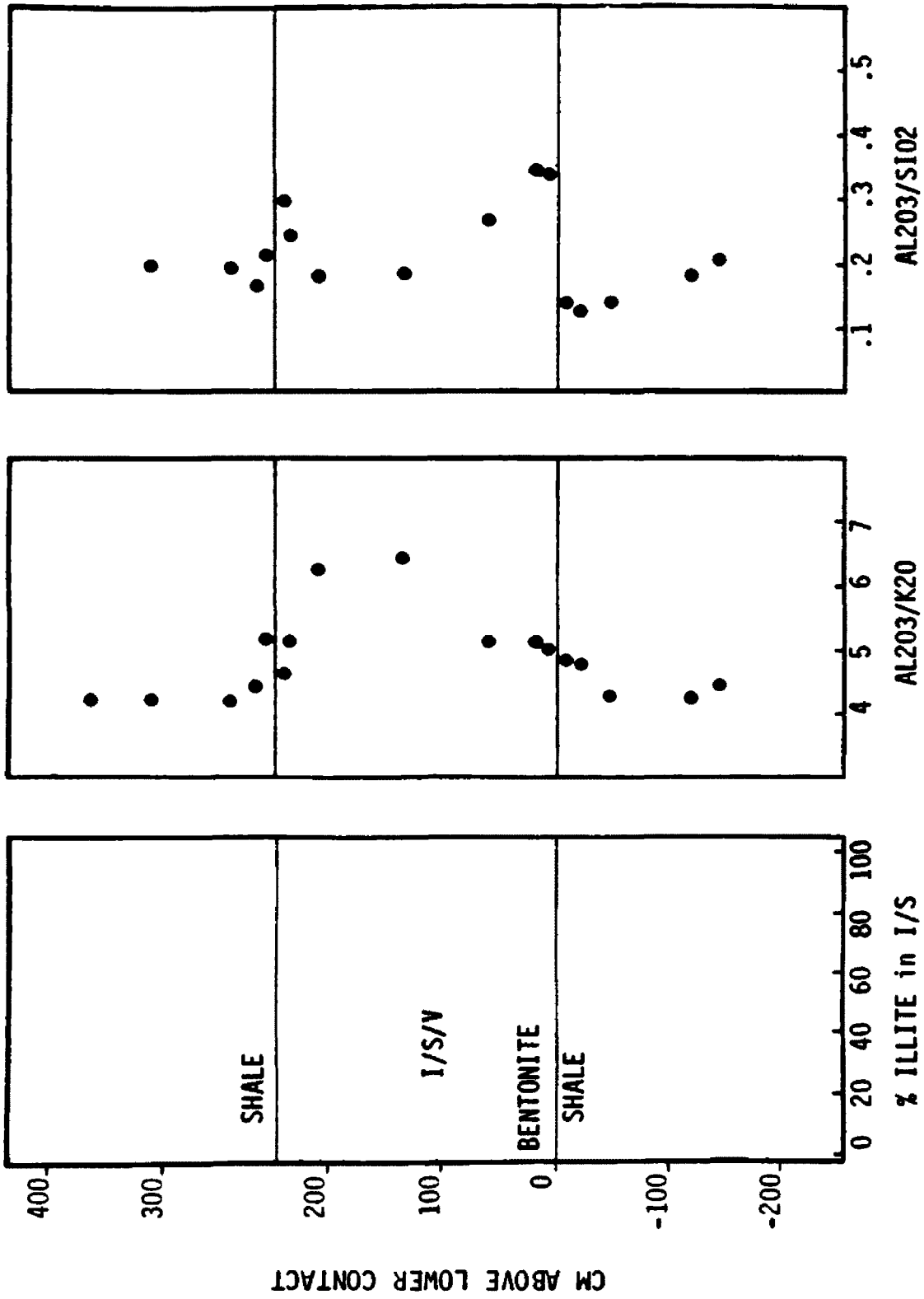Figure 6. Mineralogy and Al_2O_3/K_2O and Al_2O_3/SiO_2 for the 2.83 m thick SOUTHFORK K-bentonite

Figure 7. Mineralogy and Al_2O_3/K_2O and Al_2O_3/SiO_2 for the 2.67 m thick SUN K-bentonite

AL2O3/SIO2

AL2O3/K2O

% ILLITE in I/S

CM ABOVE LOWER CONTACT

SHALE

I/S/V

BENTONITE

SHALE

well as some discrete illite and chlorite. K_2O and SiO_2 values are higher in the shale than in the K-bentonite. K_2O does not vary across the shales, whereas SiO_2 shows an apparent enrichment approaching the K-bentonite contact.

The SUN K-bentonite (Fig. 7) shows compositional zonation of K_2O and SiO_2 similar to that found in Figure 6. However, percentage of illite layers in I/S could not be determined because XRD patterns do not match calculated patterns for any two-component M-L clay. Detailed percentage of illite in I/S in the shales could not be determined because of sample heterogeneity. However, XRD patterns of the <1 micron fraction indicate that shales contain I/S of a high percentage of illite layers (>80%) as well some discrete illite and chlorite. K_2O profiles in enclosing shales appear depleted near the K-bentonite contact, approaching values similar to those at the outer margins of the K-bentonite. SiO_2 values are higher than in the K-bentonite and decrease slightly as they approach the K-bentonite contact.

DISCUSSION

Early Alteration of Volcanic Ash to Bentonite

Variation diagrams in Figure 8 show bulk calcium, sodium and potassium plotted against percent silica for ten samples from two bentonite beds from the Sweetgrass Arch compared to the same oxides from about thirty intermediate to silicic ash flow tuff units from the Elkhorn Mountains volcanics (Rutland, 1984; Watson, 1985). It is evident that potassium and calcium, and probably sodium, are depleted in the two Arch bentonites relative to the wide range of samples from Elkhorn Mountains volcanics ashes, which I infer to be the source of the Late Cretaceous bentonites and K-bentonites of the Arch and disturbed belt. Even if the Elkhorn Mountains volcanics were not the source of the bentonites it is evident from Figure 8 that the two bentonite units are remarkably low in potassium, and somewhat low in calcium and sodium relative to silica for normal calc-alkaline igneous series (Hyndman, 1985).

The relationship of Figure 8 implies that shortly after deposition, probably as vitric ash reacted with overlying and interstitial water to form smectite, calcium and potassium, and probably sodium, were lost from the ash beds. Since I see no enrichment of these elements in the adjacent shales, it is likely that those elements were lost to the overlying water. I see no indication of early desilication of the ash beds as described by Kiersch and Keller's (1955) study of the Cheto
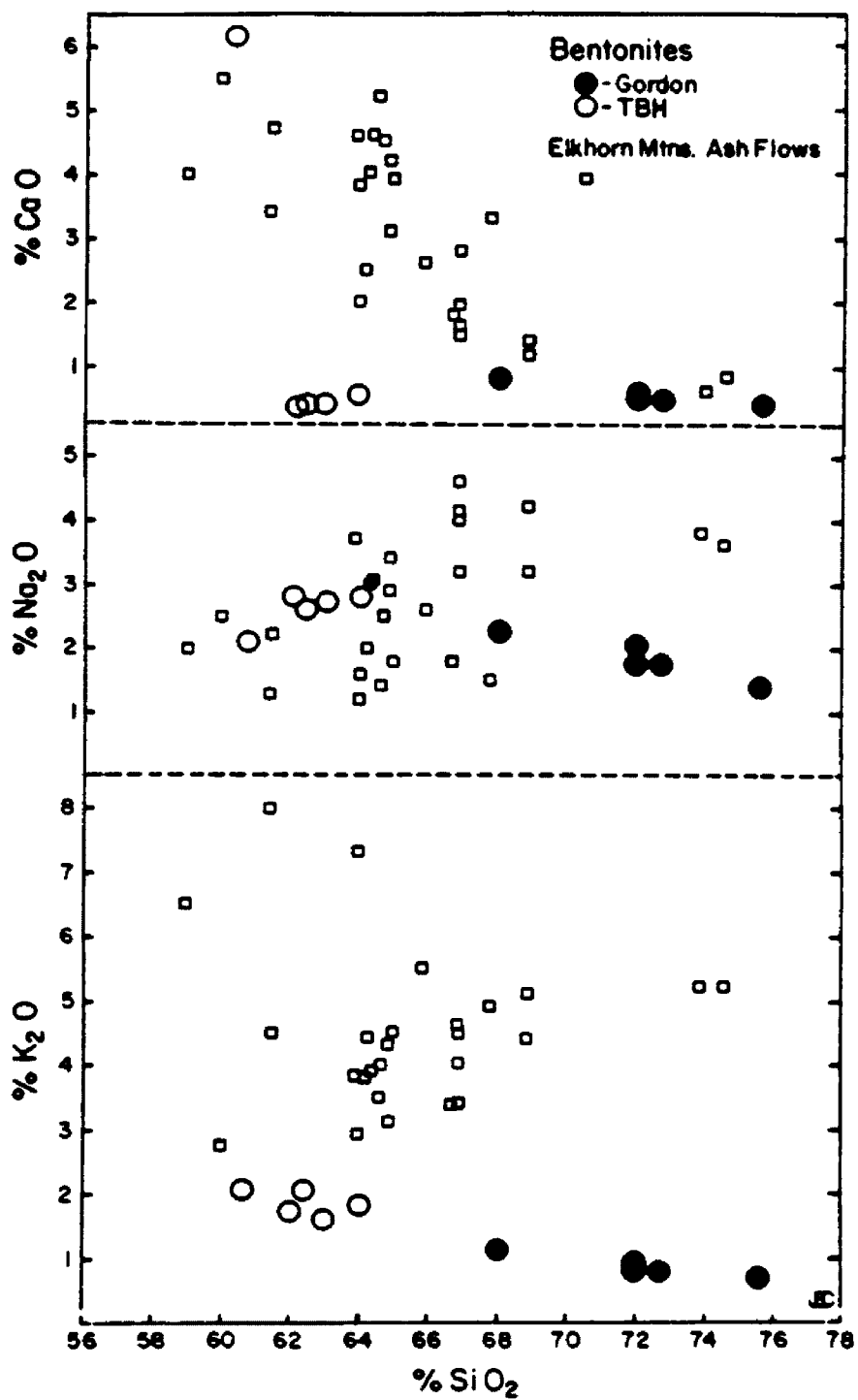
18

Figure 8 Variation Diagrams of CaO, Na_2O and K_2O versus SiO_2 for Elkhorn Mountains Volcanics and Sweetgrass Arch Bentonites

bentonite. SiO_2 values in the two Arch bentonites are equivalent to, or even higher than, those from the Elkhorn Mountains volcanics.

Sweetgrass Arch Bentonites

The TBH bentonite (Fig. 2) is typical of bentonites sampled and analyzed from the Sweetgrass Arch in that it shows little or no zoning with respect to composition or mineralogy, and consists of pure, or nearly pure, smectite. Those data are similar to results of Altaner *et al* (1984).

The GORDON bentonite (Fig. 3) is atypical of bentonites collected from the Sweetgrass Arch and unlike any described by Altaner *et al* (1984). It is mineralogically and compositionally zoned with percentage of illite layers in I/S and whole rock K_2O higher, and SiO_2 lower, at the margins of the bentonite than in the center of the bed. Altaner *et al* (1984) found this type of mineralogic and compositional zoning only in low-grade metamorphic K-bentonites of the disturbed belt and interpreted the K^+ and mineralogic trends as reflecting K^+ diffusion into the bentonite from surrounding rock units (often shales) as layer charge increases on I/S in response to low-grade metamorphism.

Layer charge on I/S most commonly increases by tetrahedral substitution of Al^{3+} for Si^{4+} in response to elevated temperatures associated with low-grade metamorphism (T=100-200°C) (Weaver and Beck, 1971; Hower *et al*, 1976). The SiO_2 distribution in the GORDON bentonite reflects diffusion out of the bed of SiO_2 that is released as a result of that process. The overall increase in layer charge in smectite is compensated for by dehydration and K^+ fixation in the interlayer site.

The reaction:

$$\text{Smectite} + Al^{3+} + K^+ \dashrightarrow \text{Illite} + SiO_2$$
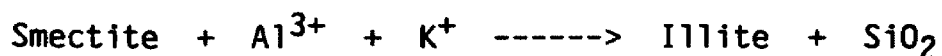
represents the progressive transformation of smectite to illite through an I/S series (Hower *et al*, 1976). Mineralogic breakdown of mica and K-feldspar in enclosing shales provide necessary K^+ for illitization to occur in bentonites (Hoffman and Hower, 1979; Altaner *et al*, 1984), however, sufficient Al^{3+} can be derived from within the smectite alone (Eberl, 1978; Boles and Franks, 1979; Roberson and Lahann, 1981; Howard and Roy, 1985).

Both of the Sweetgrass Arch bentonites have been exposed to similar burial histories involving temperatures $<<60°C$ (Hoffman and Hower, 1979). However, the TBH bentonite contains essentially pure smectite and is compositionally homogeneous, whereas the GORDON bentonite is zoned with respect to mineralogy and composition. The GORDON bentonite has a higher Al_2O_3/SiO_2 ratio and higher K_2O, MgO and total FeO concentrations than does the TBH bentonite (Table 1). I suggest that a higher Al_2O_3/SiO_2 ratio favors layer charge increase by allowing for greater Al^{3+} substitution for tetrahedral Si^{4+}. Available K^+ diffused into the GORDON bentonite to collapse the high charge smectite layers to form illite layers. Because the GORDON bentonite is mineralogically and compositionally zoned and has not been subjected to low-grade metamorphism, this is evidence that the illitization reaction may be controlled not only by reaction temperature but by bulk composition as well (Hower *et al*, 1976; Eberl, 1978; Boles and Franks, 1979; Roberson and Lahann, 1981; Inoue and Utada, 1983; Howard and Roy, 1985; Velde, 1985).

Disturbed Belt K-bentonites

As a result of low-grade metamorphism (T=100-200°C), all disturbed belt K-bentonites now show a higher percentage of illite layers in I/S and higher K_2O values than do bentonites from the Sweetgrass Arch. All thick (>1 m) K-bentonites examined show similar compositional zoning, but at least two distinct types of mineralogical trends are evident.

The compositional trends show that whole rock K_2O is higher, and SiO_2 lower, at the margins of the K-bentonites than in the centers of the beds (Figures 5-7). These trends appear to reflect K^+ diffusion into, and Si^{4+} diffusion out of the K-bentonites in response to layer charge increase in smectite resulting from low-grade metamorphism.

One of the two mineralogic trends (Figures 5 and 6) is similar to that described by Velde and Brusewitz (1982) and Altaner *et al* (1984). I/S shows a symmetric distribution about the centers of the beds with the highest percentage of illite layers in I/S at the margins of the beds and a progressive trend toward fewer illite layers near the centers of the bed.

Thick, zoned K-bentonites with illite-rich contacts and more smectite-rich middles have been interpreted as products of potassium metasomatism (Hoffman and Hower, 1979; Velde and Brusewitz, 1982; Altaner *et al*, 1984). Altaner *et al* (1984) attributed I/S compositional zonation in thick K-bentonites as reflecting progressive stages of the smectite to I/S reaction limited by the availability and slow diffusion of K^+ into the K-bentonite from surrounding shales, during low-grade metamorphism.

Howard and Roy (1985) and Chang et al (1986) demonstrated that layer charge on a smectite can increase with increasing temperature by tetrahedral substitution of Al^{3+} for Si^{4+} irrespective of the availability of K^+. Collapse of a smectite layer to form illite occurs only when K^+ is supplied to the highly charged interlayer site. In the absence of K^+ the highly charged mineral remains expanded as a smectite (dioctohedral vermiculite). Therefore, layer charge can develop independantly of the presence of K^+ and should not vary as a function of K^+ distribution. Assuming no temperature gradient across K-bentonite beds during burial metamorphism, one would expect uniformly high layer charges across K-bentonites. However, I see a distinct zoning of layer charge in I/S, as reflected by distribution of percent illite layers in I/S in Figures 3 through 6. Altaner (1985) also reported zonation of layer charges across a 2.5 m thick K-bentonite from the disturbed belt. I suggest that layer charge distribution is controlled by Si^{4+} diffusion rates out of the bed, and resulting zonation of Al_2O_3/SiO_2 ratios in the K-bentonite. Zonation of percent illite layers in I/S and K_2O are the result of zonation of Al_2O_3/SiO_2 ratios.

Excess Si^{4+} is released when Al^{3+} substitutes for Si^{4+} in the tetrahedral layer of the smectite in response to increasing temperatures. Transport of most of the Si^{4+} is through the interlayer space and into bulk solution (Lahann and Roberson, 1980). Si^{4+} then diffuses out of the K-bentonite into adjacent sediments. Because of slow diffusion rates, Si^{4+} is depleted to a larger extent from the margins of thick K-bentonites than from the centers of the beds. As a result, the Si^{4+}/Al^{3+} activity ratio is higher at the centers of thick K-bentonites than at the margins of the beds

during low-grade metamorphism. The relatively higher activity of Si^{4+} retards the illitization reaction in the center of the beds relative to the margins, producing the zonation seen.

I attribute the enrichment of silica in the shales immediately adjacent the K-bentonites of Figures 4, 6 and 7 to SiO_2 loss from the K-bentonites accompanying layer charge increase.

The shales adjacent K-bentonites (Figures 4-6) contain a relatively higher percentage of illite layers in I/S than do the K-bentonites, as well as some discrete illite and chlorite. Shales also have higher K_2O contents than the K-bentonites. However, in some shale samples near the contact with the bentonite there is a depletion of K_2O (Figures 4 and 7). Altaner et al (1984) also found progressive depletion of K_2O concentration in shales approaching both contacts of K-bentonite beds. That relationship suggests that K^+ added to the K-bentonites during low-grade metamorphism was derived from the adjacent shales. However, Altaner et al (1984) were unable to prove that K^+ was derived from K^+ mineral decomposition in adjacent shales because the Al_2O_3/K_2O ratio does not change with approach to the K-bentonite contact, indicating that similar layer silicates are present close to and far from the K-bentonite. They concluded that K^+ minerals decomposed over a larger volume of shale than sampled in the study. The Al_2O_3/K_2O ratio from shales in Figures 4 and 7 does increase approaching the K-bentonite contact. This indicates that K^+ minerals may have decomposed in adjacent shales and served as a major source of K^+ for these K-bentonites.

The one meter thick BCI K-bentonite (Fig. 4) shows a high percentage of illite

layers in I/S and little mineralogic or compositional variation. This indicates that illitization, Si^{4+} diffusion and K^+ diffusion is homogeneous, or nearly so, where distances of migration are smaller. Velde and Brusewitz (1982) and Altaner et al (1984) also found thin K-bentonites to be mineralogically and compositionally homogeneous.

The second type of mineralogical trend is shown in Figure 7. Compositionally this K-bentonite is zoned similarly to other K-bentonites. However, XRD patterns of the oriented samples of the <1 micron size fraction do not match calculated patterns for any two-component M-L clay. Figure 9 shows the responses of a typical sample from this bentonite to several treatments. K^+ saturation produces collapse of some layers, indicating some high charge layers. K^+ saturation followed by Mg^{2+} saturation and glycolation indicates that at least some of the layers that collapsed with K^+ do not re-expand upon Mg^{2+} saturation. The Mg^{2+} plus glycerol solvated sample shows less swelling than the Mg^{2+} plus glycol solvated sample, again implying that some of the expandable layers are of high charge relative to a normal smectite. The Mg^{2+} saturated sample heated to 600°C collapses to a spacing slightly below 10Å. This combination of responses to chemical and heat treatments suggests that samples from this K-bentonite bed, and others like it from the disturbed belt, consist of a single three-component ordered mixed-layer clay, and is a mixed-layer illite/smectite/vermiculite (high charge smectite).

Structural formulas calculated from chemical analyses of two apparently monomineralic <1 micron fraction samples from the TBH bentonite show layer
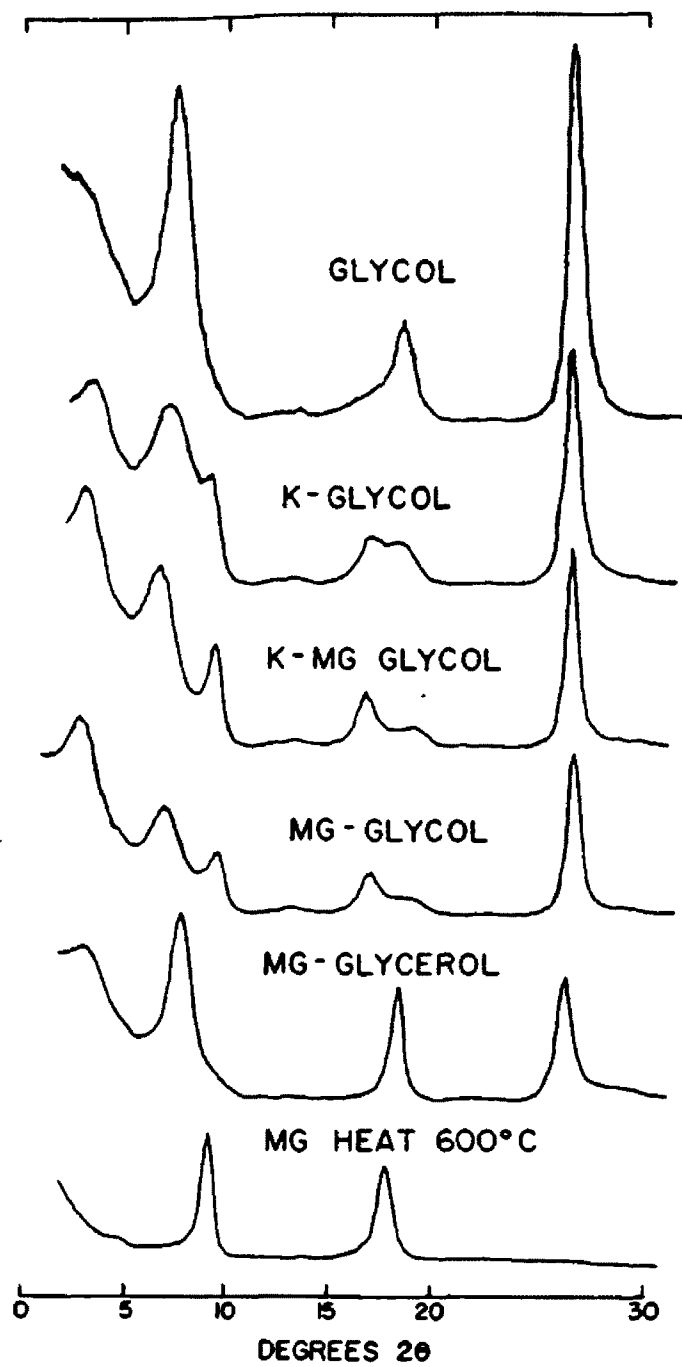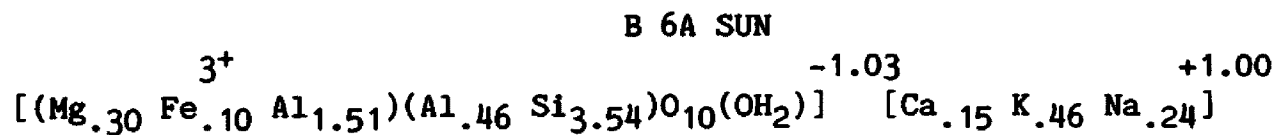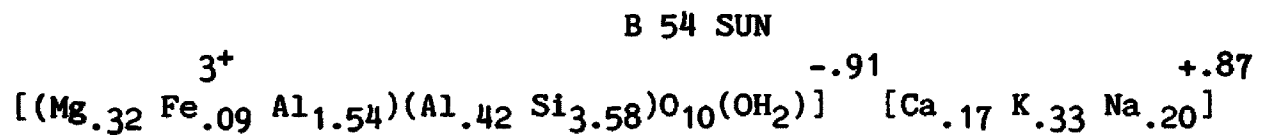
Figure 9 X-ray Patterns of a Typical Sample from the Sun K-bentonite
following several sample treatments

charges for this normal bentonite to be within normal ranges for smectites (Table 2) (Srodon *et al*, 1986). Structural formulas calculated from chemical analyses of three apparently monomineralic <1 micron fraction samples show very high layer charges for the three-component clay from the SUN K-bentonite (Table 2). Structural formulas from the SUN bed reflect a varying layer composition across the K-bentonite.

Table 2 Structural Formulas for Samples from the
Sweetgrass Arch (TBH) and Disturbed Belt (SUN)

TBH 6A

$$[(Mg_{.22} \; Fe_{.21} \; Al_{1.54})(Al_{.09} \; Si_{3.92})O_{10}(OH_2)] \quad [Ca_{.03} \; K_{.04} \; Na_{.27}]$$

3^+ $-.37$ $+.37$

TBH LS24 *

$$[(Mg_{.20} \; Fe_{.25} \; Al_{1.58})(Al_{.32} \; Si_{3.68})O_{10}(OH_2)] \quad [Ca_{.02} \; K_{.04} \; Na_{.32}]$$

3^+ $-.40$ $+.40$

B LS SUN

$$[(Mg_{.29} \; Fe_{.10} \; Al_{1.60})(Al_{.47} \; Si_{3.53})O_{10}(OH_2)] \quad [Ca_{.11} \; K_{.47} \; Na_{.08}]$$

3^+ $-.79$ $+.77$

B 54 SUN

$$[(Mg_{.32} \; Fe_{.09} \; Al_{1.54})(Al_{.42} \; Si_{3.58})O_{10}(OH_2)] \quad [Ca_{.17} \; K_{.33} \; Na_{.20}]$$

3^+ $-.91$ $+.87$

B 6A SUN

$$[(Mg_{.30} \; Fe_{.10} \; Al_{1.51})(Al_{.46} \; Si_{3.54})O_{10}(OH_2)] \quad [Ca_{.15} \; K_{.46} \; Na_{.24}]$$

3^+ -1.03 $+1.00$
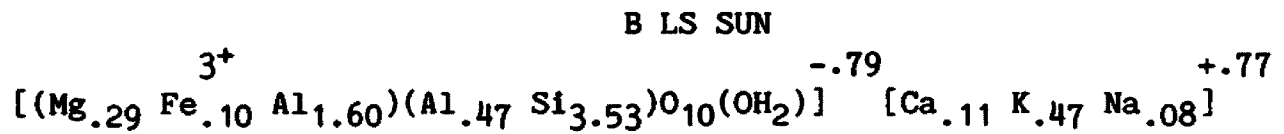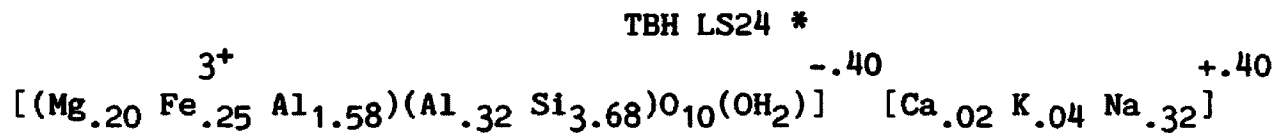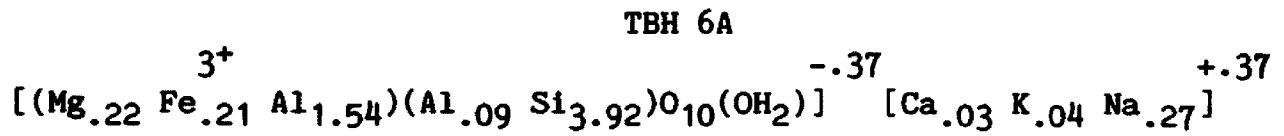
SUMMARY AND CONCLUSIONS

Bentonites from the Sweetgrass Arch and disturbed belt of western Montana were deposited as intermediate to silicic vitric volcanic ashes that altered to smectite under marine conditions. Because of early loss of alkalis the bentonites were K^+ deficient. During a thermal event (T=100-200°C) that affected the bentonites of the disturbed belt, layer charge increased on smectite in the bentonite by tetrahedral substitution of Al^{3+} for Si^{4+}. High layer charges developed even in the absence of K^+. Layer charge distribution appears to be controlled by Si^{4+} diffusion out of the bed and resulting Si^{4+}/Al^{3+} activity ratios within the K-bentonite. K-bentonites in the disturbed belt formed when K^+ diffused into the bentonite beds and collapsed high charge smectite layers to illite layers. Because Si^{4+} diffused slowly out of the bentonites, thick (>1 m) K-bentonites from the disturbed belt are zoned with illite and K-rich contacts and smectite and Si-rich inner portions. An inadequate supply of K^+ relative to the total quantity of high charge smectite layers results in three component mixed-layer clay systems consisting of illite, smectite and vermiculite (high charge smectite) in some of the K-bentonites.

Illitization appears to be controlled most strongly by reaction temperature. However, zoned bentonites from the low temperature Sweetgrass Arch (GORDON bed) suggest the reaction is also compositionally controlled. Differences in the chemical compositions of the original ash exert a fundamental influence on the

29

composition of clay minerals developed by early ash devitrification. Clay mineral compositions may then favor, or influence the development of high layer charges on smectite.

REFERENCES CITED

Altaner, S. (1985) K+ metasomatism and diffusion in Cretaceous K-bentonites from the disturbed belt, Northwestern Montana and in the Middle Devonian Tioga K-bentonite, Eastern United States, PH.D thesis., Univ. of Illinois

Altaner, S., Hower, J., Whitney, G. and Aronson, J.L. (1984) Model for K-bentonite formation : Evidence from zoned K-bentonites in the disturbed belt, Montana: Geology 12, 412-415.

Boles, J.R. and Franks, G.S. (1979) Clay diagenesis in Wilcox sandstones of Southwest Texas: implications of smectite diagenesis on sandstone cementation: Jour. Sed. Petrol. 49, 55-70.

Brindley, G.W. (1966) Ethylene glycol and glycerol complexes of smectites and vermiculites: Clays and Clay Minerals 6, 237-260.

Carroll, D. (1970) Clay minerals: a guide to their X-ray identification: Geol. Soc. Amer. Spec. Paper 126, 22-23.

Chang, H.K, MacKenzie, F.T. and Schoonmaker, J (1986) Comparison between dioctohedral and trioctohedral smectite diagenesis, Brazilian offshore basins: Clays and Clay Minerals 34, 407-423.

Eberl, D. (1977) Hydrothermal transformation of sodium and potassium smectite into mixed-layer clay: Clays and Clay Minerals 25, 215-277

Grim, R. and Guven, G. (1978) Bentonites- Geology, mineralogy, properties and uses: Developments in sedimentology 24: Elsevier Scientific Pub. Co., N.Y.

Hoffman, J. and Hower, J. (1979) Clay mineral assemblages as low-grade metamorphic geothermometers: Application to the thrust faulted disturbed belt of Montana, USA: Soc. Econ. Paleontol. Mineral. Spec. Publ. 26, 55-79.

Howard, J.J. and Roy, D.M. (1985) Development of layer charge and kinetics of experimental smectite alteration. Clay and Clay Minerals 33, 81-88.

Hower, J., Eslinger, W., Hower, M. and Perry, E.A. (1976) Mechanism of burial metamorphism of argillaceous sediments: I. Mineralogical and chemical evidence: Geol. Soc. Amer. Bull. 87, 725-737.

Hyndman, D.W. (1985) Petrology of Igneous and Metamorphic Rocks; Second Edition: McGraw-Hill Book Company, New York.

Inoue A. and Utada, M. (1983) Further investigations of a conversion series of dioctohedral mica/smectites in the Shinzan hydrothermal alteration area, northeast Japan: Clays and Clay Minerals 31, 400-412.

Jackson, M.L. (1956) Soil chemical analysis advanced course: Pub. by the author, Dept. of Soil Sciences, Univ. of Wisc., Madison, Wisc. 53706.

Lahann, R.W. and Roberson, H.E. (1980) Dissolution of silica from montmorillonite: effect of solution chemistry: Geochimica et Cosmochimica Acta 44, 1937-1943.

Kiersch, G.A. and Keller, W.D. (1955) Bleaching clay deposits, Defiance Plateau District, Arizona, Econ. Geol. 50, 469-494.

Mudge, M.R. (1970) Origin of the disturbed belt in northwest Montana: Geol. Soc. Amer. Bull. 81, 377-392.

Nascimbene, G.G. (1964) Bentonites and the Geochronology of the Bearpaw Sea, MS Thesis, University of Alberta, Canada, 80p.

Reynolds, R.C. and Hower, J. (1970) The nature of interlayering in mixed-layer illite-montmorillonites: Clays and Clay Minerals 18, 25-36.

Roberson, H.E. and Lahann, R.W. (1981) Smectite to illite conversion rates: effects of solution chemistry: Clays and Clay Minerals 29, 129-135.

Rutland, C. (1985) Geochemistry of the Elkhorn Mountains volcanics, Southwestern Montana: implication for the early evolution of a volcanic-plutonic complex: PH.D thesis, Mich. State Univ.

Slaughter, M. and Earley, J.W. (1965) Mineralogy and geological significance of the Mowry bentonite, Wyoming: Geol. Soc. Amer. Spec. Paper 83, 116.

Srodon, J. (1981) X-ray identification of randomly interstratified illite/smectite in mixtures with discrete illite: Clay Miner. 16, 297-304.

Srodon, J. (1984) X-ray powder diffraction identification of illitic materials: Clays and Clay Minerals 32, 337-349.

Srodon, J., Morgan, D.J., Eslinger, E.V., Eberl, D.D., Karlinger, M.R., (1986) Chemistry of Illite/Smectite and End-Member Illite: Clays and Clay Minerals 34, 379-384.

Van Loon, J.C. and Parissis, C.M. (1966) Scheme of silicate analysis based on the lithium metaborate fusion followed by atomic-absorption spectrophotometry: The Analyst 94, 1057-1062.

Velde, B. and Brusewitz, A.M. (1982) Metasomatic and non-metasomatic low grade metamorphism of Ordovician metabentonites in Sweden. Geochimica et Cosmochimica Acta 46, 447-452.

Velde, B. (1985) Possible chemical controls on I/S composition during diagenesis: Mineralogic Magazine 49, 387-391.

Watson, S.M. (1986) The Boulder batholith as a source for the Elkhorn Mountains volcanics, southeast quarter of the Deerlodge 15' quadrangle, Southwestern Montana: MS thesis, Univ. of Montana.

Weaver, C.E. and Beck, K.C. (1971) Clay water diagenesis durial burial metamorphism: how mud becomes gneiss: Geol. Soc. Amer. Spec. Paper 134, 96.